ChemComm

Geometric and redox flexibility of pyridine as a redox-active ligand that can reversibly accept one or two electrons

Journal:	*ChemComm*
Manuscript ID:	CC-COM-07-2014-005495.R1
Article Type:	Communication
Date Submitted by the Author:	01-Aug-2014
Complete List of Authors:	Lewis, Richard; Yale University, Department of Chemistry MacLeod, K.; Yale University, Department of Chemistry Mercado, Brandon; Yale University, Department of Chemistry Holland, Patrick; Yale University, Department of Chemistry

Geometric and redox flexibility of pyridine as a redox-active ligand that can reversibly accept one or two electrons

Richard A. Lewis,[a] K. Cory MacLeod,[a] Brandon Q. Mercado,[a] and Patrick L. Holland*[a]

Received (in XXX, XXX) Xth XX 200X, Accepted Xth XX 200X
First published on the web Xth XX 200X
DOI: 10.1039/b000000x

A low-coordinate iron(I) species can reversibly reduce pyridine, either by one electron to give a new C-C bond, or by two electrons to give a pyridine-derived bridge with an unprecedented μ-η^1:η^3 binding mode.

Pyridine-derived ligands can accept negative charge, and an example is the ability of $[Ru^{II}(bpy)_3]^{2+}$ to separate charge in its excited state $[Ru^{III}(bpy)_3(bpy^{\bullet-})]^{2+}$.[1] The ground state of these complexes can also have significant radical anion character on the pyridine ligands.[2-4] The strong bond between the oxidized metal and the reduced pyridine is important for enabling this transfer of electrons, because reduction of free pyridine is very difficult in the absence of a metal (-2.7 V vs. SCE).[5] We have been interested in showing the potential for the parent pyridine to accept charge, and exploring the ways in which the pyridine responds to this additional charge. We reported in 2012 that L'Fe(*tert*-butylpyridine)$_2$ (L' = 2,4-bis(2,6-diisopropylimino)pentyl; see Figure 1) is not described well using the formal iron(I)-pyridine formulation, but requires a significant contribution from a resonance structure L'Fe(py)(py$^{\bullet-}$) with iron(II) and a reduced pyridine.[6] In this trigonal-pyramidal complex, unpaired spin density lay preferentially on the basal pyridine. When the pyridine had no *tert*-butyl group, the radical character on the basal pyridine led to the rapid, reversible formation of a C-C bond between two basal pyridines to form a bimetallic species with two iron(II) ions and a bridging dianionic ligand (Scheme 1). This dimer was present only in the solid state, and the monomer was present in solutions (no solution could be made concentrated enough to fully characterize the dimer in solution). A related reversible Yb-phenanthroline coupling was recently reported in which both monomer and dimer could be observed in solution, enabling the thermodynamics of the C-C bond to be measured quantitatively.[7]

Here, we report that decreasing the size of the supporting ligand on iron from L' to L (L = 2,4-bis(2,6-dimethylimino)-3-methylpentyl) enables the quantitative characterization of the elusive monomer-dimer equilibrium. Further, the smaller ligand also gives a surprising new way for pyridine to accept two electrons, showing the great flexibility of pyridine in its ability to accept charge and undergo bond distortion, formation, and cleavage.

The source of the iron(I) fragment LFe in this chemistry is the π-benzene complex LFe(C_6H_6). The benzene ligand in this complex is labile; for example, we recently reported that benzene can be replaced by CO and xylyl isocyanide.[8] Pyridine, on the other hand, does not react with LFe(C_6H_6) in benzene solution because pyridine binds more weakly than benzene. Therefore, all of the following studies were performed in aliphatic or ethereal solvents, where it was possible to displace benzene. In Et_2O solution, the addition of 2.1 equiv of pyridine to LFe(C_6H_6) immediately yields a red/brown solution from which complex **1** can be isolated in 72% yield as a red powder. Complex **1** crystallizes in the orthorhombic space group *Pca*2$_1$. Two crystallographically independent molecules are observed in the unit cell for **1**.

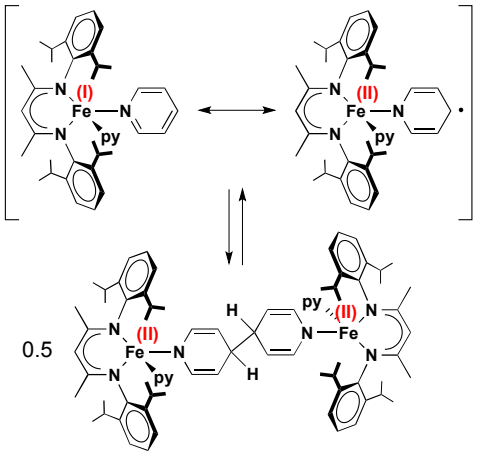

Scheme 1. Published interconversions using L', a larger β-diketiminate supporting ligand with isopropyl substituents.[6]

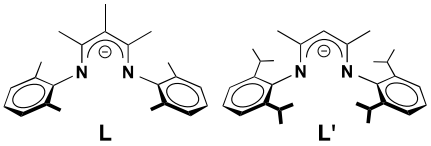

Figure 1. Ligands used in this study.

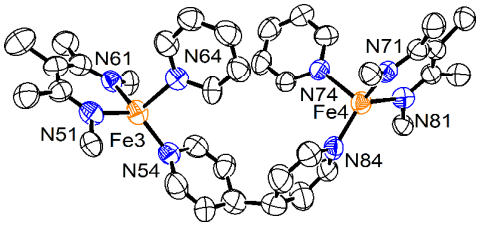

Figure 2. Thermal-ellipsoid plot (50%) of **1**$_2$, with xylyl groups and hydrogens omitted for clarity. Only one of the two independent molecular sites is shown. The other site consists of 58% of **1**$_2$ and 42% of **1**$_1$.

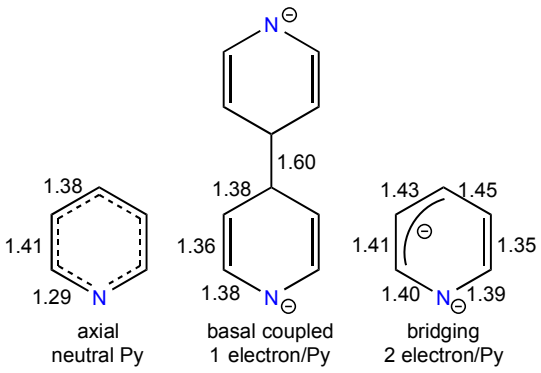

Figure 3. Interatomic distances in different pyridine ligands.

Both correspond primarily to a dimeric pyridine-coupled product (**1$_2$**) that is analogous to the previously reported complex L'Fe(Py)($N_2C_{10}H_{10}$)(Py)FeL'.[6] (A secondary disorder component will be discussed below.) The geometry about each iron in **1$_2$** is distorted trigonal pyramidal, with the unmodified pyridines in the axial positions. The Fe–N bond lengths to the chelating β-diketiminates (Fe–N = 1.961(8) – 1.984(8) Å) are consistent with those in other high-spin iron(II) diketiminate complexes in the literature.[9] The Fe–N bond lengths to the basal coupled $N_2C_{10}H_{10}$ moiety in **1$_2$** are 1.931(9) and 1.958(9) Å, which are close to the Fe-N distance in its L' analogue (1.942(3) Å), and are significantly shorter than the Fe–N bond lengths of 2.103(8) and 2.111(8) Å to the axial pyridines. The short Fe-N bonds to the coupled pyridines suggest that these N atoms are best viewed as negatively charged amido groups as part of a $N_2C_{10}H_{10}^{2-}$ fragment. The bond lengths within the pyridine rings (Figure 3, center) are also consistent with C=C double bond localization in the bridging ligand.

The view of **1$_2$** as having reduced pyridine implies that the iron atoms are oxidized from the iron(I) oxidation state in the precursor LFe(C_6H_6). This idea was supported by the Mössbauer spectrum of solid **1$_2$** at 80 K, which shows the predominant component to have an isomer shift of δ = 0.76 mm/s and a quadrupole splitting of $|\Delta E_Q|$ = 1.35 mm/s. These values are close to those in the previously reported (L'FePy)$_2$(μ-$C_{10}H_{10}N_2$) with δ = 0.77 mm/s and $|\Delta E_Q|$ = 1.57 mm/s.[6] The isomer shifts are characteristic of four-coordinate high-spin iron(II) β-diketiminate complexes (δ = 0.69-0.90 mm/s and $|\Delta E_Q|$ = 1.32-3.12 mm/s).[9, 10]

One of the two sites in the asymmetric unit of the crystal has disorder, and the secondary (42%) component fits best to two nearby *uncoupled* LFe(pyridine)$_2$ molecules, which we abbreviate **1$_1$**. This monomer comes from a monomer/dimer equilibrium that was previously proposed in the L' analogues,[6] though in that case the monomer could be observed in the solid state only when a *tert*-butyl group was used to prevent dimerization.[5] ^{1}H NMR spectra of **1** in C_6D_{12} suggest that the monomer and dimer are in an equilibrium that is slow on the NMR time scale, because two distinct sets of peaks are observed for **1$_1$** and **1$_2$**, but the equilibrium is established within minutes of mixing the solutions. Dissolving LFe(C_6H_6) in *tert*-butylpyridine gives a set of peaks analogous to **1$_1$** without formation of a set analogous to **1$_2$**, and the observation of only monomer when the *para* position is blocked supports our interpretation of the solution behavior of **1**. Interestingly, using pyridine-d_5 as the solvent favors **1$_2$** over **1$_1$**. We attribute this shift in the equilibrium to a solvent effect, because it takes place only at concentrations of pyridine near and above 1 M, where pyridine becomes a major component of the solvent (see ESI).

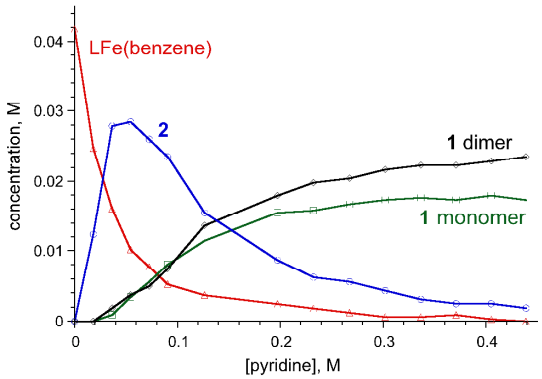

Figure 4. Dependence of the concentration of different species on the amount of pyridine added to LFe(C_6H_6) in THF-d_8 solution at RT. Solid lines have been added between points for guidance. Concentrations are based on ^{1}H NMR integrations *versus* a capillary standard, and have a ±5% uncertainty limit.

Lowering the temperature of a pyridine-d_5 solution of **1** to -30 °C favors **1$_2$**, and raising it to 80 °C favors **1$_1$**. The shift between dimer and monomer is also consistent with a color change from red at low temperature (**1$_2$**) to green at room temperature (**1$_1$**), as previously observed with L'. Fitting the ratio of ^{1}H NMR integrations at a variety of temperatures yields thermodynamic parameters $\Delta H°$ = -25 ± 3 kJ/mol and $\Delta S°$ = -85 ± 8 J/mol•K for the conversion of **1$_1$** to **1$_2$**. Thus the bond dissociation enthalpy of the new C-C bond in **1$_2$** is weaker than the one in Gomberg's dimer of triphenylmethyl radicals (48 kJ/mol)[11] and similar to the recently reported ytterbium-phenanthroline complex in THF (24 kJ/mol).[7]

This behavior of the LFe-derived pyridine complexes displays similarities to those previously reported for L'Fe analogues. However, more significant differences emerge at relatively low pyridine concentrations between 0.0182 mM and 0.405 mM in solution, where an additional paramagnetic iron species (**2**) is observable in ^{1}H NMR spectra. The maximum concentration of **2** is achieved at [py] = 0.0545 mM in THF-d_8 (Figure 4). Its ^{1}H NMR spectrum is most consistent with two inequivalent β-diketiminate environments, each having averaged C_{2v} symmetry on the NMR time scale.

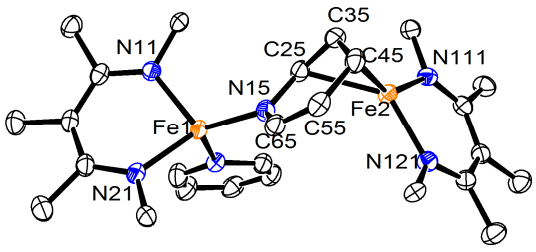

Figure 5. Thermal-ellipsoid plot (50%) of **2**, with xylyl groups and hydrogens omitted for clarity.

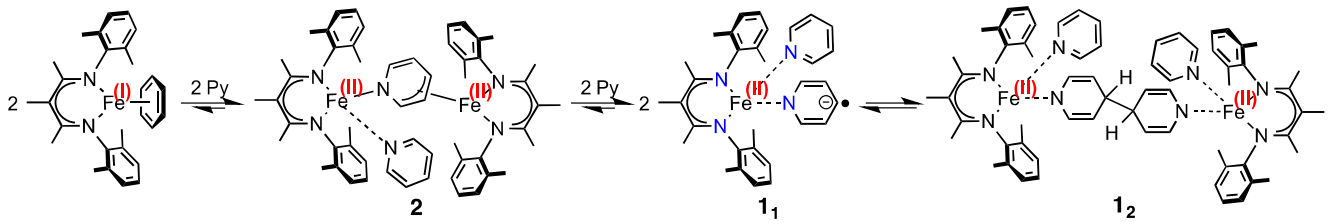

Scheme 2. Reversible pyridine binding and reduction in this system depends on the amount of pyridine added.

Crystallization from Et_2O gave **2** in 30% isolated yield. (The isolated yield is not representative of the solution speciation, because ^{1}H NMR spectroscopy with an internal standard indicates ~80% conversion to **2** in solution under similar conditions.) Its X-ray crystal structure (Figure 5) shows the difference between the two iron environments that is evident by ^{1}H NMR spectroscopy (see above). One (Fe1) is tetrahedral, and is bound by a chelating β-diketiminate (Fe–N = 1.9780(2) and 1.9946(2) Å), one terminal pyridine ligand (Fe–N = 2.1099(2) Å), and one bridging pyridine ligand (Fe–N = 1.9513(2) Å). All four *ortho*-methyl groups on each diketiminate have the same chemical shift, and since N-C(aryl) rotation is generally slow in iron β-diketiminate complexes,[12] this implies that the terminal pyridine is exchanging rapidly, such that it samples both sides of the diketiminate on the NMR time scale. The Fe–N bond distance to the bridging pyridine is 0.15 Å shorter than the other pyridine, which suggests that this nitrogen has a formal negative charge as an amido group, as shown in the right side of Figure 3.

The other iron atom in **2** (Fe2) has significantly shorter distances to the β-diketiminate (Fe–N = 1.9463(2) and 1.9490(2) Å). It interacts in a η^3 fashion (Fe–C = 1.976(2) – 2.245(2) Å) with the bridging pyridine molecule. A closer analysis of the C-C bond lengths within the bridging pyridine (Figure 3) gives additional support for the assignment as a pyridine dianion. The C-C bond lengths between the C atoms bound to Fe2 are 1.41-1.43 Å, whereas the other C-C bonds are 1.445(3) and 1.352(3), indicating localized C-C single and double bonds, respectively (Figure 3). The two C-N distances within the ring are near 1.40 Å, which is characteristic of a C-N single bond and much longer than the distances in pyridine (~1.35 Å).[13] The π-allyl interaction also causes bending of the bridging pyridine ring by 26.0° between the allyl plane and the NCC plane. This μ–η^1:η^3 binding mode of a doubly reduced pyridine has not been reported previously. It is different than other multinuclear complexes with doubly reduced pyridines; for example, Gambarotta has reported PDI complexes in which a reduced pyridine interacts with Cr or Fe through an η^5 interaction.[14, 15]

The Mössbauer spectrum of **2** collected at 80 K has two quadrupole doublets with very similar intensities, corresponding to the two different iron environments. One has δ = 0.76 mm/s and $|\Delta E_Q|$ = 1.66 mm/s. The similarity in parameters to **1** suggests that this signal corresponds to the tetrahedral Fe1, which has similar coordination and similarly has one pyridine reduced to an anionic ligand. The other signal has δ = 0.67 mm/s and $|\Delta E_Q|$ = 1.29 mm/s, which is also consistent with an iron(II) formulation. Having a second iron(II) gives additional support to the assignment of a doubly reduced bridging pyridine ligand.

In conclusion, the accumulated experiments here support the coupled equilibria shown in Scheme 2. In this reaction manifold, two different types of geometric and electronic rearrangements are available to pyridine ligands. Despite these changes in the bonding within the bridging pyridine units, the species can interconvert at room temperature within minutes. These compounds demonstrate the varied ways that pyridine can behave as a redox-active ligand, and give perspectives on potential metal binding modes that could be accessed in photosensitizers and other species where redox of pyridine complexes is important.

Notes and references

[a] *Department of Chemistry, Yale University, 225 Prospect St., New Haven, CT 06520 USA; E-mail: patrick.holland@yale.edu*

† Electronic Supplementary Information (ESI) available: experimental, crystallographic, and computational details. See DOI: 10.1039/b000000x/

‡ This work was supported by the National Institutes of Health (Grant GM065313).

1 A. Juris, V. Balzani, F. Barigelletti, S. Campagna, P. Belser and A. von Zelewsky, *Coord. Chem. Rev.*, 1988, **84**, 85.
2 W. Kaim, *Inorg. Chem.*, 2011, **50**, 9752.
3 C. C. Scarborough and K. Wieghardt, *Inorg. Chem.*, 2011, **50**, 9773.
4 M. Wang, J. England, T. Weyhermueller, S.-L. Kokatam, C. J. Pollock, S. DeBeer, J. Shen, G. P. A. Yap, K. H. Theopold and K. Wieghardt, *Inorg. Chem.*, 2013, **52**, 4472.
5 L. Meites and P. Zuman, *CRC Handbook Series in Organic Electrochemistry*, CRC Press, Cleveland, 1977.
6 T. R. Dugan, E. Bill, K. C. MacLeod, G. J. Christian, R. E. Cowley, W. W. Brennessel, S. Ye, F. Neese and P. L. Holland, *J. Am. Chem. Soc.*, 2012, **134**, 20352.
7 G. Nocton, W. W. Lukens, C. H. Booth, S. S. Rozenel, S. A. Medling, L. Maron and R. A. Andersen, *J. Am. Chem. Soc.*, 2014, **136**, 8626.
8 K. C. MacLeod, D. J. Vinyard and P. L. Holland, *J. Am. Chem. Soc.*, 2014, **136**, 10226.
9 R. E. Cowley, J. Elhaïk, N. A. Eckert, W. W. Brennessel, E. Bill and P. L. Holland, *J. Am. Chem. Soc.*, 2008, **130**, 6074.
10 R. E. Cowley, E. Bill, F. Neese, W. W. Brennessel and P. L. Holland, *inorg chem*, 2009, **48**, 4828.
11 K. Ziegler and F. Ditzel, *Justus Liebigs Annalen der Chemie*, 1929, **473**, 194.
12 P. L. Holland, T. R. Cundari, L. L. Perez, N. A. Eckert and R. J. Lachicotte, *J. Am. Chem. Soc.*, 2002, **124**, 14416.
13 F. H. Allen, *Acta Cryst.*, 2002, **B58**, 380.
14 I. Vidyaratne, J. Scott, S. Gambarotta and R. Duchateau, *Organometallics*, 2007, **26**, 3201.
15 J. Scott, I. Vidyaratne, I. Korobkov, S. Gambarotta and P. H. M. Budzelaar, *Inorg. Chem.*, 2008, **47**, 896.